

This is the author's accepted manuscript. The final published version of this work (the version of record) is published by Sage in *The Holocene* (201x) available at:
doi:xxxx.xxxxxx/xxxxxxxxxxxxxx

The manuscript was accepted for publication on 11/08/2018.

This work is made available online in accordance with the publisher's policies. Please refer to any applicable terms of use of the publisher. The complete bibliographic reference is:

Fyfe RM, Woodbridge J, Palmisano A, Bevan A, Shennan S, Burjachs F, Legarra Herrero B, García Puchol O, Carrión J, Revelles J and Roberts N (201x) Prehistoric palaeodemographics and regional land cover change in eastern Iberia *The Holocene* xx, xxx-xxx

Prehistoric palaeodemographics and regional land cover change in eastern Iberia

Fyfe, R.M.¹, Woodbridge, J.¹, Palmisano, A.², Bevan, A.², Shennan, S.², Burjachs, F.³, Legarra Herrero, B.², García Puchol, O.⁴, Carrión, J.S.⁵, Revelles, J.⁶, Roberts, N.¹

1 School of Geography, Earth and Environmental Sciences, University of Plymouth, Plymouth, PL4 8AA, UK

2 Institute of Archaeology, University College London, 31-34 Gordon Square, London, WC1H 0PY, UK

3 ICREA Barcelona, Catalonia, Spain; Rovira i Virgili University (URV), Tarragona, Catalonia, Spain; Institut Català de Paleoeologia Humana i Evolució Social (IPHES), Campus Sescelades URV, W3, 43007 Tarragona, Spain

4 PREMEDOC Research Group, Departament de Prehistoria, Arqueologia i Història Antiga, Universitat de València, Avenida Blasco Ibañez 28, 46010, València, Spain

5 Departamento de Biología Vegetal, Facultad de Biología, Universidad de Murcia, 30100 Murcia, Spain

6 Departament de Prehistoria, Universitat Autònoma de Barcelona, 08193 Bellaterra, Spain

Abstract

Much attention has been placed on the drivers of vegetation change on the Iberian Peninsula. Whilst climate plays a key role in determining the species pools within different regions and exerts a strong influence on broad vegetation patterning, the role of humans, particularly during prehistory, is less clear. The aim of this paper is to assess the influence of prehistoric population change on shaping vegetation patterns in eastern Iberia and the Balearic Islands between the start of the Neolithic and the late Bronze Age. 3385 radiocarbon dates have been compiled across the study area to provide a palaeodemographic proxy (radiocarbon summed probability distributions: SPD). Modelled trends in palaeodemographics are compared with regional-scale vegetation patterns deduced from analysis of 30 fossil pollen sequences. The pollen sequences have been standardised with count data aggregated into contiguous 200-yr time windows from 11000 cal. yr BP to present. Samples have been classified using cluster analysis to determine the predominant regional land cover types through the Holocene. Regional human impact indices and diversity metrics have been derived for northeast and southeast Spain and the Balearic Islands. The SPDs show characteristic boom-and-bust cycles of population growth and collapse, but there is no clear synchronism between northeast and southeast Spain other than the rise of Neolithic farming. In northeast Iberia patterns

35 of demographic change are strongly linked to changes in vegetation diversity and human impact
36 indicator groups. In the southeast increases in population throughout the Chalcolithic and early
37 Bronze Age result in more open landscapes and increased vegetation diversity. The demographic
38 maximum occurred early in the 3rd millennium cal. BP on the Balearic Islands and is associated with
39 highest levels of human impact indicator groups. The results demonstrate the importance of
40 population change in shaping the abundance and diversity of taxa within broad climatically-
41 determined biomes.

42

43 **Keywords**

44 Radiocarbon SPD, palaeodemographics, prehistory, pollen, land cover, human impact, diversity,
45 Spain, Holocene

46

47

48 **INTRODUCTION**

49

50 Much attention has been placed on Holocene vegetation change, and on the drivers of that change,
51 in the Iberian Peninsula. Much of that focus has been on the role of climate in determining
52 vegetation trajectories, particularly in regions where moisture availability is a key factor in the
53 macroecological patterning exhibited by more arid regions (Carrión et al., 2010b). Climate inevitably
54 does play an important role in influencing and determining the species present across different
55 regions (Carrión et al., 2010a), and climatic change can exert a strong influence on broad vegetation
56 dynamics. For example, many pollen sequences describe an increase in mesic woodland associated
57 with a relatively wetter mid-Holocene phase (e.g. Carrión et al., 2001a, 2001b; Carrión et al., 2004;
58 Carrión et al., 2007; Aranbarri et al., 2014). Increasing aridity then resulted in expansion of
59 sclerophyllous and xeric communities (Carrión et al., 2010; Pérez-Obiol et al., 2011). The role of
60 humans in influencing vegetation change, particularly in earlier archaeological periods, is by contrast
61 less straightforward, especially at the regional level. In more recent periods, since 1500 cal. yr BP,
62 the influence of anthropogenic forcing on vegetation in eastern Iberia can be clearly demonstrated
63 and linked to increasing land degradation caused by grazing pressure (Carrión et al., 2001a; Carrión
64 et al., 2004; Aranbarri et al., 2014). In addition, research over the last few years has also uncovered
65 increasing evidence for the impact of earlier societies on land cover in eastern Iberia. According to
66 Carrión et al. (2010a) human settlement and land use has played a role in shaping vegetation
67 patterns since the mid-Holocene through land conversion for agriculture, mining, and grazing. For
68 example, Revelles et al. (2015) describe pronounced changes in deciduous woodland cover and
69 maintenance of cleared landscapes from the early Neolithic in northeast Spain, in close proximity to
70 known early Neolithic archaeological settlements. It is likely that whilst climate controlled broad
71 geographical patterning on vegetation (e.g. by controlling fundamental species distribution and
72 influencing competition between species), this was overprinted by human disturbances, at least at
73 the local scale (Castro et al., 1994, 1998). There is thus a need to further explore the role of past
74 populations on land cover change.

75

76 Radiocarbon dates from archaeological sites are increasingly used as proxies for past demographic
77 change, through the use of summed probability distributions (radiocarbon SPD, also known as
78 summed calibrated date probability distributions: SCDPD, Shennan et al., 2013). The basis of the
79 approach is summarised in several places (e.g. Shennan and Edinborough, 2007; Shennan et al.,
80 2013; Palmisano et al., 2017) and assumes that change in the number of radiocarbon dates in a
81 defined region is a useful proxy for demographic trends. Balsera et al. (2015b) presented the first

82 attempt at prehistoric palaeodemographics using radiocarbon dates for the whole of Iberia, drawing
83 on 4402 dates from 1167 archaeological sites. They identified the characteristic ‘boom and bust’
84 cycle of population growth and subsequent contraction at the start of the Neolithic (c.7250 cal. yr
85 BP) observed elsewhere in Europe (Shennan et al., 2013). Subsequent studies have applied the
86 approach in the Iberian peninsula (e.g. Bernabeu et al., 2014; García Puchol et al., 2015). Lillios et al.
87 (2016) explored regional trends in demographic change from three sub-regions of the Iberian
88 Peninsula (northwest, northeast and southeast) using dates from settlements and burials across the
89 Chalcolithic and Bronze Age and García Puchol et al. (2017) mapped spatial and temporal patterns in
90 radiocarbon SPD to show dynamics of the final hunter gatherers and the first farmers. These studies
91 noted clear differences in regional demographic trends, but record increases in population as
92 inferred from the radiocarbon SPD in spite of inferred increases in aridity during the sixth and fifth
93 millennia cal. BP. These sub-regional inferences are extended by Blanco-González et al. (2018), who
94 suggest inter-regional differences in climate as a potential explanatory variable for regional
95 demographic differences. The characteristically mediterranean southeast and northeast regions are
96 described as having small demographic responses to known climate events (e.g. the 4.2 ka cal BP
97 event) in comparison to regions more influenced by Atlantic climatic conditions. Blanco-González et
98 al. (2018) call for further regional work in Iberia on subsistence economies, demographic trends and
99 ecological transformations, signalling that understanding past land cover and demographic change is
100 a priority research area.

101

102 The aim of this paper is to test how far regional vegetation changes and ecological transformation
103 within eastern Iberia can be explained by archaeologically-derived records of prehistoric
104 demographic change. Regional trends in vegetation through the Holocene will be derived from
105 synthesis of multiple pollen sequences, and inter-regional comparisons made between the northern
106 and southern regions. Data from the Balearic Islands will also be compared to the mainland: islands
107 are useful as experimental laboratories where it can be shown they are isolated from human impact.
108 Current evidence suggests that the Balearic Islands of Mallorca and Menorca were not settled until
109 around 4320 cal. yr BP (Burjachs et al., 2017; Pérez-Jordà et al., 2018). Following colonisation the
110 Balearic Islands are connected to Iberia but are a distinct region. Data from these islands can thus
111 provide valuable reference conditions for natural (pre-human colonisation) vegetation dynamics,
112 and for exploring the impact of known settlement and population expansion trends.

113

114 **METHODOLOGY AND MATERIALS**

115

116 ***Palaeo-demographic data***

117

118 Prehistoric demographic data is inferred from a summed probability distribution approach utilising
119 radiocarbon dates as surrogates for population (Shennan et al., 2013). Radiocarbon dates from
120 archaeological sites were compiled from existing online databases and electronic and print
121 publications (Martínez et al., 1997; Manen and Sabatier, 2003; Weninger et al., 2009; Van Strydonck
122 and de Roock, 2011; Hinz et al., 2012; Aranda Jiménez et al., 2015; Balsera et al., 2015a, 2015b;
123 Manning et al., 2015; Lillios et al., 2016; Oms et al., 2016; Paulsson, 2017; Vermeersch, 2017). Dates
124 are stored in a georeferenced database following Palmisano et al. (2017). A total of 3885
125 uncalibrated radiocarbon dates from 814 sites have been collected. All the radiocarbon dates are
126 from archaeological contexts, with the majority being samples of bone, charcoal and wood.
127 Radiocarbon dates obtained from marine samples such as shell are not included to avoid the
128 complicated issues arising from unknown or poorly understood marine reservoir offsets. Fewer than
129 20 dates have standard deviations greater than 300 years. Biases caused by multiple dates from the
130 same archaeological phase at a site are accounted for by aggregating uncalibrated radiocarbon dates
131 from the same site that are within 100 years of each other and dividing by the number of dates that
132 fall in this bin (Timpson et al., 2014). The probabilities from each calibrated date are combined to
133 produce a summed probability distribution (SPD). The resulting summed probabilities are binned
134 into 200-year time windows to match the time windows used in the analysis of pollen sequences.
135 Archaeological periods are defined from literature, but it should be noted that archaeological
136 periodisation for the Balearic Islands is distinct from the Iberian mainland. All dates are given in
137 calibrated years before present (cal. yr BP). The timing of archaeological periods varies across
138 mainland Iberia, but broadly the first Neolithic cultural material is dated to 7550-7450 cal. yr BP, and
139 the peninsula experienced a rapid transition process from the Mesolithic to the Neolithic (García
140 Puchol et al., 2009; López de Pablo and Gómez Puche, 2009; García Puchol and Salazar-García, 2017).
141 Neolithic culture was established across northeast Spain by 7250 cal. yr BP (Oms et al., 2018). The
142 subdivisions of Antolín et al. (2015) are used for the Neolithic periods: early Neolithic (7350-6450 cal.
143 yr BP), middle Neolithic (6450-5150 cal. yr BP) and late Neolithic/Chalcolithic (5150-4250 cal. yr BP);
144 the start of the late Neolithic is slightly later in southeast Spain. The Bronze Age is divided into three
145 periods following Lull et al. (2013): early Bronze Age (4250-3500 cal. yr BP); late Bronze Age (3500-
146 3250 cal. yr BP) and final Bronze Age (3250-2850 cal. yr BP).

147

148 It is not currently possible to use radiocarbon date distributions as a reliable palaeodemographic
149 proxy after the end of the Bronze Age as the number of available dates for this period is too low:

150 relative dating via cultural material gradually replaces radiocarbon in the development of site
151 chronologies. Iberia came into contact with the Phoenicians and Greeks during the Iron Age (from
152 the 9th century BC, ~2700 cal. yr BP) and colonies such as *Emporion* on the coast of Catalonia were
153 established (founded in 2475 cal. yr BP). This brought eastern Iberia into the realm of written
154 history. Carthaginian colonies such as Cartagena came under Roman rule following the 2nd Punic
155 War (late 3rd century BC, ~2200 cal. yr BP). The Romans dominated the Iberian Peninsula until the
156 5th century AD (1500 cal. yr BP). After a period of Visigothic rule, almost the whole of eastern Iberia
157 was conquered by Islamic Moors soon after ~700 AD (1250 cal. yr BP). The Christian conquest was a
158 slow process, not completed until the fall of Granada in 1492 AD (458 cal. yr BP). Both Moslem and
159 Christian Medieval periods saw a significant growth in population in Iberia and laid the economic
160 foundations of the modern Spanish state.

161

162 ***Modern and fossil pollen datasets***

163

164 Pollen count data from the European modern (Davis et al., 2013) and fossil pollen databases (EPD
165 version Oct. 2017: Leydet, 2007-2017) were combined with additional fossil records provided by a
166 network of data contributors to compile a dataset of 257 fossil records and 1798 modern pollen
167 surface samples spanning the Mediterranean region. Pollen sequences with reliable chronologies
168 (Giesecke et al., 2014) were selected for analysis and new sediment core chronologies were
169 constructed for additional records using the ‘bacon’ R package (Blaauw & Christen, 2011). The pollen
170 count data from each site were summed into 55 contiguous 200-year time windows between the
171 periods 11000 and -65 cal. yr BP. Descriptions of the methodological approaches developed and
172 applied to the pollen datasets are provided in Woodbridge et al. (2018) and Fyfe et al. (2018) along
173 with detailed information on the harmonisation of the pollen taxonomy. The approach has allowed
174 the identification of key vegetation types across the Mediterranean region as a whole. This paper
175 draws on a sub-set of 30 fossil sequences from 27 pollen sites and 112 modern surface samples for
176 Mediterranean Spain (Figure 1).

177

178 ***Palaeoclimate datasets***

179

180 The closest and most complete non-palynological proxy-based records for which data are available
181 from eastern Iberia are used as palaeoclimate indicators for comparison with radiocarbon SPD and
182 pollen-inferred land cover and indices. Datasets have been normalised around their mean and
183 standard deviation to produce z-scores as described in detail in Finné et al. (in review). For

184 northeast Spain a multiproxy record of lake level and salinity has been used from Lake Estanya
185 (Morellón et al., 2009). The lake level record from Laguna de Medina (Reed et al., 2001) is used for
186 southeast Spain. There is no published proxy-climate dataset currently available from the Balearic
187 Islands.

188

189 ***Pollen data analysis***

190

191 An unsupervised data-driven approach was used to assign pollen samples to vegetation cluster
192 groups for all modern and fossil sites within the Mediterranean (Fyfe et al., 2018; Woodbridge et al.,
193 2018). The approach is based on the similarity of assemblages using Ward's hierarchical
194 agglomerative clustering method (Ward, 1963). Analysis was undertaken using the 'Rioja' R package
195 (Juggins, 2015). A phytosociological classification approach was used to identify the frequent and
196 abundant pollen taxa within each cluster group based on its median and interquartile range (IQR).
197 Interpretive name descriptors were given to each vegetation cluster using the phytosociological
198 classification tables along with comparisons with other classification systems, land cover types
199 defined by remote sensing and the results of previous studies (see Woodbridge et al., 2018).

200

201 Non-metric multidimensional scaling (NMDS) was applied to the Spanish fossil datasets (using taxon
202 percentage data aggregated into 200-year time windows) to explore major patterns. NMDS was run
203 using the 'vegan' R package (Oksanen et al., 2016). Data were square-root transformed, and
204 dissimilarity was calculated using Bray-Curtis. Simpson's diversity index (Simpson, 1949) was
205 calculated for each pollen sample and aggregated by region. Three pollen indicator groups were
206 used to summarise key changes in the datasets and identify possible human impact in the records.
207 This included: (a) the average non-arboreal pollen sum (%NAP); (b) the OJC index (sum of *Olea*,
208 *Juglans*, *Castanea*), an established Mediterranean tree-crop indicator group (Mercuri et al., 2013a);
209 and the anthropogenic pollen index (API: sum of *Artemisia*, *Centaurea*, Cichorioideae and *Plantago*,
210 cereals, *Urtica* and *Trifolium* type) proposed by Mercuri et al. (2013b). For the OJC index the taxon
211 Oleaceae was grouped with *Olea*. Analysts have routinely separated taxa within the Oleaceae family
212 (e.g. *Fraxinus*, *Phillyrea*); Oleaceae is considered most likely to represent poorly-preserved *Olea*.
213 *Artemisia* is included within the API to facilitate comparison with results from other Mediterranean
214 regions, and the value of the API more broadly is discussed later.

215

216 **RESULTS**

217

218 ***Palaeodemographic change in eastern Iberia***

219

220 The summed probability distribution (SPD) for radiocarbon dates for all 3885 dates (1438 sites) are
221 shown on Figure 2a. Deviations above or below a null model based on a simple theoretical model of
222 population growth and plateau are highlighted, indicating periods with population growth or decline
223 outside a 95% envelope of the long-term logistic trend. An increase in population is inferred at the
224 start of the Neolithic at 7500 cal. yr BP and the whole of the sequence between 7500 and 6000 cal.
225 yr BP is above the logistic range. The population trend departs significantly over the long-run from a
226 logistic model of population growth (p-value 0.001) at 5600-5300 (end of the Middle Neolithic) and
227 5000-4700 cal. yr BP inferring population decline. Between these periods the trend indicates
228 population increase at the start of the late Neolithic/Chalcolithic (around 5300-5000 cal. yr BP).
229 Further significant increases in population occur from the early Bronze Age (Argaric period in
230 southeast Spain, c. 4100 cal. yr BP) with population declining towards the start of the late Bronze
231 Age (at 3500 cal. yr BP). Significant population increases occur during the late Bronze Age (at 3200
232 cal. yr BP) and during the final Bronze Age (3000 cal. yr BP). There are insufficient dates within the
233 Iron Age (after 2500 cal. yr BP) for meaningful interpretations.

234

235 Regional divergences from the Eastern Iberia dataset are shown on Figures 2b-d. Northeast Spain
236 includes 1076 radiocarbon dates from 376 sites. We assess to which degree the demographic
237 patterns of each sub-region depart from the pan-regional trend via a permutation test following
238 Crema et al. (2016). This method statistically assesses differences between the SPD of radiocarbon
239 dates within each sub-region and the overall pan-regional average. Population is significantly above
240 the overall pan-regional average throughout the Neolithic, with notable increases at the start of the
241 Neolithic (at 7500 cal. yr BP) followed by a small decline towards the end of the early Neolithic (at
242 6700 cal. yr BP). A population increase is visible at the start of the late Neolithic/Chalcolithic period.
243 The Bronze Age SPD is significantly below that of the whole dataset, and by the Iron Age the time
244 series starts to become unreliable. There is an increase during the early Bronze Age (from 4000 cal.
245 yr BP) and a decline at the start of the late Bronze Age.

246

247 In southeast Spain, the 1219 dates from 306 sites largely follow the general background SDP trends,
248 with the exception of a statistically-significant positive deviation (a population increase and greater
249 than the pan-regional average) at the start of the Neolithic, and a significant negative deviation
250 (population decrease and lower than the pan-regional average) during the middle Neolithic (6100-
251 5900 cal. yr BP). SDP-inferred population is significantly higher throughout the late

252 Neolithic/Chalcolithic and the early Bronze Age. SPD-inferred population rises steadily, with the
253 peak in population recorded around 3700 cal. yr BP. Significantly lower populations are inferred
254 from the late Bronze Age on.

255

256 For the Balearic Islands 1590 radiocarbon dates from 778 sites are used (Figure 2D). The Balearic
257 Islands have a much later date for the start of farming than mainland Iberia, and were the last major
258 Mediterranean islands to be colonised (Burjachs et al., 2017). Prior to the Bronze Age the islands are
259 believed to be uninhabited. Step-wise increases in the SPD are recorded during the late Neolithic (at
260 4800 cal. yr BP), at the start of the early Bronze Age (4200 cal. yr BP) at the start of the late Bronze
261 Age (3400 cal. yr BP) and during the final Bronze Age (3000 cal. yr BP). From 3400 cal. yr BP the SDP
262 for the Balearic Islands is above the pan-regional trend.

263

264 ***Pollen clusters: synthesis***

265

266 The 27 pollen sites used in the analysis are divided into three groups (Figure 1; Table 1), covering
267 northeast Spain (7 sites), southeast Spain (12 sites) and the Balearic Islands (8 sites). The results of
268 the hierarchical clustering are presented on Figure 3. The clusters follow the division of
269 Mediterranean pollen assemblages into the 16 groups described in detail in Woodbridge et al.
270 (2018). Not all clusters described by Woodbridge et al. (2018) are represented in the Spanish pollen
271 datasets. The main clusters identified in the Spain pollen are 1.1 (sclerophyllous parkland), 1.3
272 (steppe parkland), 4.0 (pine forest), 5.1 (pine woods) and 5.2 (pine steppe). The pine clusters are
273 differentiated on the basis of the proportions of pine and the co-occurring taxa within each group.
274 Other groups of note include 1.2 (evergreen shrubland: Oleaceae) and 6.1 (deciduous oak woods).
275 There are clear temporal changes in the representation of the clusters. Sclerophyllous parkland and
276 pine woods are dominant from 11000-9000 cal. yr BP. From 9000 cal. yr BP pine forest and pine
277 steppe both increase, co-incident with decline in pine woods. From 8000 cal. yr BP sclerophyllous
278 parkland declines whilst the number of sites classified as steppe parkland increase. Between 9000-
279 3400 cal. yr BP deciduous oak woods are recognised, but not outside of this time period, and alder
280 woods (8.1) are recognised between 4800-3200 cal. yr BP. Evergreen shrubland (Oleaceae) becomes
281 continuously recognised around 5200 cal. yr BP, declining after 2400 cal. yr BP but rising in the last
282 millennium. Pine steppe has a step-wise increase at 4800 cal. yr BP, and steppe parkland rises at
283 3000 cal. yr BP. The pine forest group is not recognised after 1400 cal. yr BP.

284

285 There are insufficient pollen sites within the northeast and southeast mainland regions to make
286 proportions of clusters in each time window meaningful. Comparison between the Balearic Islands
287 and the mainland show that on the mainland sclerophyllous scrub is limited to the early Holocene
288 (pre-8000 cal. yr BP). In contrast sclerophyllous scrub dominates and persists on the Balearic Islands.
289 The Balearic Islands have a very restricted number of cluster groups, with evergreen shrubland
290 (Oleaceae) from 5800 cal. yr BP, and steppe parkland not appearing until after 2000 cal. yr BP. Pine
291 groups are only sporadically recognised, with pine steppe best represented between 4800-2000 cal.
292 yr BP.

293

294 ***Analysis of pollen data***

295

296 The low numbers of pollen sites in each mainland region make comparison of the cluster-based
297 results difficult because when cluster results are amalgamated for a region values can be highly
298 influenced by individual sites. Regional differences in vegetation patterns are thus explored using
299 non-metric multidimensional scaling. Performing NMDS with three axes resulting in a stress of
300 0.175. Biplots of taxon scores for axes 1 and 2 and axes 1 and 3 are shown on Figure 4, with taxa
301 grouped by broad ecological meaning (sclerophyllous taxa, non-sclerophyllous arboreal taxa, the OJC
302 group (plus *Vitis*), the API group, and other herbaceous taxa). Taxa in the OJC group plot together in
303 the ordination space, close to the centre of the plot. The API taxa are widely dispersed along axis 1,
304 but are tightly grouped on axis 2 (Figure 4a). The exception is *Plantago lanceolata* that lies distant
305 from all other taxa, low on axis 2. There is no clear separation between sclerophyllous and non-
306 sclerophyllous taxa on either biplot, and herbaceous taxa are widely dispersed. These patterns are
307 likely to be a function of the highly heterogeneous nature of Mediterranean vegetation.

308

309 Biplots of site scores for each 200-year time window show groupings of sites from 9900-100 cal. yr
310 BP (Figure 5a,b; labelled version in Supplementary Information). The plots show a clear separation
311 between the Balearic Islands and the mainland sites for most of the Holocene, with the sites on the
312 Balearic Islands inhabiting the upper left quadrant. Between 9900-4900 several mainland sites plot
313 within the same ordination space as the Balearic Island records, demonstrating similar pollen
314 assemblages (Antas, San Rafael and Elx). Creixell remains grouped within the Balearic sites
315 throughout the entire period. From 6300-5300 cal. yr BP a distinct grouping of sites occurs in the
316 lower left quadrant of the biplots. This includes the high elevation sites in southeast Spain (Baza,
317 Gador, Siles, Sabinar and Villaverde) but also includes the mid-elevation site at Navarrés and the
318 northeast Spain site Lake Banyoles. Beyond the grouping of the Balearic Islands sites and the high

319 elevation sites there are no other clear groupings in the dataset that persist through time. Mainland
320 sites from the southeast and northeast occupy similar areas of the biplots (e.g. see biplots for 6900
321 and 3300 cal. yr BP).

322

323 The difference in position of site across the three NMDS axes (chord distance) between adjacent
324 time intervals is used as an estimate of the rate of change in pollen assemblages. Values are
325 averaged for each region to examine region-scale drivers of vegetation change (demographic and
326 climatic change). These mean chord distances are shown on Figure 6 alongside key pollen indices
327 (NAP sum, the OJC and API indices and Simpson's diversity index), the radiocarbon SPD and regional
328 climate records. Low values for mean NMDS chord distances imply stability in vegetation, whilst
329 higher values indicate greater changes in assemblages between time windows. In northeast Spain
330 NMDS chord distance scores show distinct increases starting at 7500 cal. yr BP (peak at 7100 cal. yr
331 BP), at 5100 cal. yr BP (peak at 4500 cal. yr BP) and at 3100 cal. yr BP. Between these peaks values
332 return to low levels implying stable vegetation between time windows. The increase at 7500 cal. yr
333 BP is coincident with increases in the NAP sum, a rise in Simpson's diversity index and the first peak
334 in the radiocarbon SPD. The rise in mean NMDS chord distance score at 5100 cal. yr BP is coincident
335 with an increase in radiocarbon SPD values. The rise in mean NMDS chord distance score at 3100
336 cal. yr BP corresponds with an increase in NAP sum, the first continuous OJC index curve and an
337 increase in the API. The Simpson's diversity score suggests that diversity is highest from 6000 cal. yr
338 BP, with greatest diversity at 500 cal. yr BP.

339

340 The summary metrics for southeast Spain indicate a much higher NAP sum compared to northeast
341 Spain during the early Holocene (around 40% for southeast Spain compared to 20% for the
342 northeast sequences). The API also shows high levels, in excess of 10% during the early Holocene
343 when human impact should be minimal. The mean NMDS chord distances show some suggestion of
344 cyclic behaviour over millennial timescales, but peaks are more muted than in northeast Spain.
345 Peaks occur around 9100, 7500, 6300, 4100 and 700 cal. yr BP. The most notable change in the
346 indices is an increase in the NAP sum from around 5500 cal. yr BP, which is coincident with a small
347 step-increase in the API index, a major rise in the Simpson's diversity index and the major increase in
348 the radiocarbon SPD. The Simpson's diversity index falls to low levels at 2300 cal. yr BP from a peak
349 at 3500 cal. yr BP. It then increases again, peaking at 1500 cal. yr BP, coincident with a second
350 increase in the NAP sum.

351

352 In the Balearic Islands, the mean NMDS chord distance is highest at the start of the records (at 8700-
353 8300 cal. yr BP) and drops to 'baseline' values centred around 0.4. This is much higher than values
354 for northeast and southeast Spain, which have baselines around 0.2. An isolated peak in mean
355 NMDS chord distance scores for the Balearic Islands occurs at 2900 cal. yr BP, with increasing scores
356 from 3500 cal. yr BP. The peak coincides with the maximum radiocarbon SPD value. Neither the OJC
357 nor API trends bear any relationship to the radiocarbon SPD. The Simpson's diversity scores are
358 broadly stable but decline from 3500 cal. yr BP.

359

360 ***Correlation between palaeodemographics, palaeoclimate and pollen-based indices***

361

362 Correlation matrices for each region, for key pollen indicators shown on Figure 6, radiocarbon SPD
363 and regional climatic records are given on Tables 2-4. Correlation is assessed using Spearman's Rank
364 Correlation Coefficient (R-values) and statistically-significant results ($p < 0.05$) are highlighted. In
365 northeast Spain significant positive correlations are found between radiocarbon SPD and the NMDS
366 chord distance, NAP sum and OJC index. The NAP sum is also positively correlated with the OJC
367 index, API and Simpson's diversity. Simpson's diversity is also positively correlated with the OJC
368 index. In southeast Spain the radiocarbon SPD is negatively correlated with the OJC index, and
369 positively correlated with Simpson's diversity. Simpson's diversity is also positively correlated with
370 the NAP sum, but negatively correlated with the OJC index. In the Balearic Islands radiocarbon SPD
371 is positively correlated with the NAP sum, the OJC index and Simpson's diversity, even major
372 changes in demographics and pollen indices do not appear to align (Figure 6). The NAP sum is
373 positively correlated with the OJC and API, and OJC index with Simpson's diversity.

374

375 **DISCUSSION**

376

377 ***Palaeodemographic trends in eastern Iberia, 10000-2500 cal. yr BP***

378

379 Clear palaeodemographic changes are seen in eastern Iberia through the compilation of
380 archaeological radiocarbon dates and the production of summed probability distributions (Figure
381 2a). The start of the Neolithic across the whole study region is clearly marked by a step-wise
382 increase in the summed probability distributions at 7500 cal. yr BP. This accords well with the
383 established timing of the Mesolithic/Neolithic transition in eastern Iberia (García Puchol et al., 2009;
384 Fernández-López de Pablo and Gómez-Puche, 2009; García Puchol and Salazar-García, 2017; Oms et
385 al., 2018). There are regional differences between the north and south study areas, with a more

386 abrupt increase in the northeast, and a more gradual, and marginally earlier, increase in the
387 southeast. Oms et al. (2018) suggested full expansion of the Neolithic in the northeast was
388 marginally delayed from the littoral locations favoured by the first Neolithic areas. The significant
389 demographic expansion in Figure 2 agrees with general radiocarbon-based models of population
390 growth across Iberia as a whole (Balseira et al., 2015b) and in more detailed regional analyses that
391 shows the earliest Neolithic population expansion in the east of the peninsula (Drake et al., 2017). In
392 the northeast (Figure 2b) a decline in the SPD around 6700 cal. yr BP implies a 'bust' following the
393 demographic boom of the earlier Neolithic, a feature also recognised by Drake et al. (2017) in their
394 regional analysis, and a pattern that follows trends identified in temperate Europe (Shennan et al.,
395 2013). The pattern is replicated in the southeast with a shorter boom phase. The causes of the
396 boom and bust phenomena in Europe remain unclear, but a longer Neolithic 'boom' in the north
397 east might reflect more successful agrarian strategies in the less arid northern regions around the
398 Ebro valley and the foothills of the Pyrenees.

399

400 The pattern of radiocarbon-inferred population demographics for southeast Spain from the late
401 Neolithic/Chalcolithic to the late Bronze Age is similar to that of Lillios et al. (2016). Lillios et al.
402 (2016) do not observe major deviations from a null model based on logistic growth for the
403 southeast, and observe pronounced differences between population trends in the southeast,
404 southwest and northwest. In the southeast settlement aggregation is observed in landscape survey
405 and excavation (Blanco-González et al., 2018), and it is widely accepted that populations increased
406 by up to as much as three times from late Neolithic levels with the development of the Argaric
407 Bronze Age society in southeast Iberia (Aranda Jiménez et al., 2014). The results show a long period
408 growth that peaks around 4000 cal. yr BP. Lillios et al. (2016) do not present radiocarbon SPD from
409 the northeast across the late Neolithic/Chalcolithic and Bronze Age, but the region is included in the
410 synthesis of Blanco-González et al. (2018). Our results confirm those of Blanco-González et al. (2018)
411 and indicate strong interregional differences in SPD-inferred demographic patterns: the major
412 increases and declines in population in the southeast are not reflected in patterns in the northeast.
413 Within the northeast the late Neolithic/Chalcolithic is characterised by continuity in cultural practice
414 (including subsistence, settlement and technology) until c.4400 cal. yr BP (Blanco-González et al.,
415 2018), although increases in the radiocarbon SPD do not occur until 4000 cal. yr BP (Figure 2a).

416

417 The precise timing of the first settlement on the Balearic Islands is not well defined (Burjachs et al.,
418 2017), but unequivocal evidence for human presence exists from the late Neolithic/Chalcolithic
419 period (Ramis et al., 2002). From 4300-3800 cal. yr BP sedentary cultures are well known. No

420 published radiocarbon SPD for the islands is known. The pattern in Figure 2d shows a small increase
421 at 4700 cal. yr BP signalling early but low levels of cultural material, followed by increasing
422 population levels after 4200 cal. yr BP. Radiocarbon-inferred populations continue to increase
423 through the Bronze Age reaching a peak in the Iron Age (c.2500 cal. yr BP) and are associated on the
424 easternmost Balearic Islands (Mallorca and Menorca) with the indigenous Talaiotic Culture. Pérez-
425 Jordà et al. (2018) indicate that the earliest settlers came with a complete agricultural package,
426 including domesticated animals, cereals and legumes, with strong similarities to the Catalanian
427 (northeast) subsistence traditions.

428

429 ***Human impact on vegetation dynamics in eastern Iberia***

430

431 Assessing human drivers of vegetation change in Mediterranean regions is confounded by the
432 multiple potential factors that can cause vegetational change, in particular climatic variations
433 (Carrión, 2002). There has also been much debate over the role of climate in cultural and
434 demographic change within Iberia (e.g. Fernández-López de Pablo and Gómez-Puche, 2009;
435 Bernabeu et al., 2016; Blanco-González et al., 2018), implying that separation of these drivers of land
436 cover change may be difficult. In spite of this the strong demographic signals that have emerged
437 from the synthesis of radiocarbon dates can be compared to transformed pollen data to assess the
438 extent to which population changes can explain changes in palaeovegetation patterns.

439

440 ***Northeast Spain***

441

442 The results from northeast Spain indicate a significant correlation between the radiocarbon-inferred
443 palaeodemographics and key human impact indicators (Table 2, Figure 6a). Increased population
444 levels are associated with higher total NAP values, suggesting increasing levels of open ground, and
445 the correlation with the OJC index implies higher levels of tree cropping associated with higher
446 population levels. This does not mean taxa within the OJC group are domesticated early in
447 Prehistory, and previous work does not demonstrate full domestication of these taxa until the third
448 millennium cal. yr BP (Rodríguez-Ariza and Montes Moya, 2005). Prehistoric societies are likely to
449 have transformed vegetation to promote such useful wild resources (e.g. Rowley-Conwy and Layton,
450 2011). The positive relationship between demographic increases and rates of change is consistent
451 with human transformation of land cover in response to higher population levels. There are
452 insufficient pollen sites to evaluate changes in the dominant land cover types (clusters) between the
453 northeast and southeast of Iberia; however, the overall pattern from the mainland sites shown on

454 Figure 3 implies fragmentation of pine-dominated vegetation communities and an expansion of pine
455 steppe (cluster 5.2), particularly from 5000 cal. yr BP, and steppe parkland (cluster 1.3) during the
456 earlier Neolithic period. Recent links between cultural transitions and climatic change have been
457 made (e.g. Cortés-Sánchez et al., 2012, Bernabeu Aubán et al., 2016), and episodes of abrupt climate
458 change such as the 4.2 ka cal BP event have been linked to changing land use strategies and
459 population levels (Blanco-González et al., 2018). More favourable climatic conditions may have been
460 one of a series of factors that promoted population expansion, presumably as a consequence of
461 improved agrarian conditions. The Neolithic archaeobotanical datasets demonstrate permanent
462 fields rather than shifting cultivation (Antolín et al., 2015). Gathering of wild food through the
463 Neolithic period indicates intensive but sustainable exploitation of both domesticated and wild
464 resources (Antolín and Jacomet, 2015), a pattern also seen in other parts of Europe (e.g. Bevan et al.,
465 2017).

466

467 It is not possible to compare pollen-inferred land cover changes with archaeologically-inferred
468 population levels after ~2500 cal. yr BP. However, the main pollen classification changes after this
469 time involved tree crops and anthropogenic indicators rather than overall tree cover. Most of the
470 Holocene decline in arboreal pollen in northeast Iberia occurred during prehistoric rather historic
471 times, notably between 7300 and 2500 cal. yr BP. This process of forest loss was almost certainly
472 multi-causal, but the results presented here indicate that human agencies potentially contributed to
473 this process soon after the arrival of Neolithic farming.

474

475 *Southeast Spain*

476

477 In contrast to the correlations between past population and vegetation indices in the northeast
478 there are no statistically significant positive relationships observed in the southeast, other than
479 between population levels and vegetation diversity. Increased openness in the landscapes (i.e.
480 higher NAP values) also results in greater diversity, although this correlation (+0.337) is not
481 statistically significant. This pattern can be expected if a greater degree of openness signifies a
482 greater number of different vegetation communities. Previous work at the European scale has
483 indicated latitudinal gradients in diversity, with highest diversity levels in the most southern regions
484 of Europe and this pattern has previously been observed using Holocene pollen data (Silvertown,
485 1985). The significant negative relationship between OJC and demographics demonstrates, at least
486 in part, the difficulty in separating wild from domesticated taxa. Finds of wild olive in Iberia have
487 been recognised during the Neolithic (Antolín and Jacomet, 2015), but intensification of olive

488 production for trade does not begin until the Roman period in eastern Spain (Terral and Arnold-
489 Simard, 1996, and see Langgut et al., in review). The value of these human impact indices, including
490 the API, is thus questionable in this sub-region. Many of the indicator taxa used are characteristic of
491 disturbed open ground, and *Artemisia* can also be a strong indicator of arid conditions. These are
492 exactly the conditions that are found in southeast Spain through the early Holocene, a region which
493 includes the most arid part of Europe. In the analysis for southeast Spain, the API shows high values
494 at the start of the Holocene (Figure 6), reducing to their lowest values before climbing again from
495 around 6000 cal. yr BP. It seems logical to interpret increases in the API with human impact,
496 particularly as after 7500 cal. yr BP; however, this is clearly a complex indicator group that includes
497 natural disturbance factors including fire and climatic factors, such as aridity.

498

499 In spite of the lack of correlation between NAP sum and radiocarbon SPD across the whole record in
500 southeast Spain, the major rise of population from the Chalcolithic to the late Bronze Age (between
501 5500-3500 cal. yr BP) is strongly aligned with increases in these openness indicators, and this
502 appears to strongly control vegetation diversity. The NMDS chord distance indicates greater change
503 in vegetation assemblages through this period also. The increase in population levels by possibly up
504 to three times through the Argaric period thus had a major impact on vegetation character in the
505 region. Per capita human impact also increased at the start of Bronze Age, as metallurgy led to
506 exploitation of Iberia's abundant mineral resources. Mining and copper/bronze smelting has been
507 reported from the start of the 5th millennium BP (Murillo-Barroso et al., 2017), but the major
508 increases in production associated with the Argaric culture would have led to increased use of wood
509 fuel, and hence in deforestation. The imprint of Chalcolithic and Argaric culture population and
510 economic rise can be seen in the mean NAP sum in the southeast Spanish pollen records, which
511 declined progressively between 5000 and 3700 cal. yr BP. It also led to a shift from pine
512 forests/woods (clusters 2 and 3) to more open pine steppe (cluster 6). The demographic collapse
513 during the late Bronze Age (from 3500 cal. yr BP) only led to a temporary reversal in the
514 trajectory of vegetation change. There was a minor re-expansion of arboreal vegetation between
515 3600 and 3000 cal. yr BP. The limited scale of vegetation recovery may be a consequence of
516 degradation of the landscape through grazing, combined with higher aridity, resulting in bioclimatic
517 limits to the growth of woody vegetation (Carrión et al., 2007; Pérez-Obiol et al., 2011). It is not
518 possible to compare human population trends and pollen-inferred land cover change after ~2500
519 cal. yr BP using the data presented here. However, in many pollen records from southeast Spain, it
520 is precisely at this point in time that large-scale human transformation of vegetation cover becomes
521 clearly detectable, for example at Mar Menor on the coast of Murcia (Azuara, 2018).

522

523 *Balearic Islands*

524

525 Several important contributions discuss both the general vegetation history (Burjachs et al., 2017)
526 and patterns of land use (Pérez-Jordà et al., 2018) in the Balearic Islands. Burjachs et al. (2017)
527 established that groups of islands have differences in their vegetation histories, notably between the
528 eastern Gymnesian islands (Mallorca and Menorca) versus the western Balearic Islands of Ibiza and
529 Formentera. These broad patterns are supported by the analysis presented here. Changes in
530 vegetation assemblages between 6000 and 5000 cal. yr BP in the overall cluster-based analysis
531 (Figure 3c) have been attributed to regional climatic change by Burjachs et al. (2017). This might
532 explain increases in the NAP sum, and the OJC index from 6000 cal. yr BP (Figure 6), reflecting a
533 cooling trend and increasing aridity limiting growth of mesic woodland. This demonstrates the
534 sensitivity of vegetation in the western Mediterranean to natural climatic variability, at least through
535 the early to mid-Holocene. Comparison of pollen indices against continuous proxy-based climate
536 records from the Balearic Islands is currently not possible owing to a lack of published regionally-
537 relevant climate records (see Finné et al., in review, for a more complete discussion on
538 Mediterranean climate and teleconnections).

539

540 Strong positive correlations between the radiocarbon SPD and human impact indicator groups (NAP
541 sum and OJC) are a result of the rank-order correlation approach used: the highest values of
542 demographics coincide with the highest levels of NAP and the OJC index, although the patterns are
543 not immediately obvious from the curves presented (Figure 6C). Once again, the utility of indices of
544 human impact that are based on naturally-occurring taxa, particularly those whose abundances
545 relate to a wide variety of disturbance processes, is questionable for periods before demonstrable
546 human impact. Pérez-Jordà et al. (2018) do not find strong evidence for *Olea* cultivation on the
547 Balearic Islands until the Iron Age. *Olea* is present and can be locally abundant in the sclerophyllous
548 vegetation of the islands, as such it has been argued that consumption could be a result of gathering
549 of wild fruits (and see Langgut et al., in review).

550

551 **CONCLUSIONS**

552

553 The synthesis of pollen data and comparison with a proxy for palaeodemographics demonstrates
554 regional differences in the impact of population change on vegetation across eastern Iberia and the
555 Balearic Islands. In northeast Iberia patterns of demographic change are strongly linked to changes

556 in vegetation diversity and human impact indicator groups. In the more arid southeast relationship
557 patterns in human impact indicator types and past population demographics are less clear, but the
558 rise in population through the Chalcolithic and early Bronze Age Los Millares and Argaric cultures
559 results in more open landscapes and increased vegetation diversity. Vegetation diversity decreases
560 as population levels fall, but the landscape remains open, presumably as a result of soil degradation
561 and increasing aridity into the late Holocene. On the Balearic Islands, prior to initial human
562 colonisation, climate was the primary pacemaker of vegetation in the early and middle Holocene.

563

564 There was no clear synchronism between demographic trends in the three sub-regions of eastern
565 Iberia between 10000 and 2500 cal. yr BP, other than the rise in population on the mainland at the
566 start of Neolithic farming ~7600-7300 cal. yr BP. In northeast Iberia population grew rapidly after
567 this time and stayed high, whereas in southeast Spain the main demographic rise occurred much
568 later (after 5300 cal. yr BP) and population subsequently declined (after 3500 cal. yr BP). While
569 regional population in southeastern Spain peaked soon after the start of the Argaric culture, on the
570 Balearics the demographic maximum occurred early in the 3rd millennium cal BP, during the early
571 Iron Age Talaiotic Culture. As we can assume that these three sub-regions experienced a broadly
572 similar climatic history, it can be inferred that climate changes were not the main pacemaker for
573 long-term demographic trends for eastern Iberia as a whole, even though they must have
574 contributed to societal changes in a variety of ways. For example, the 4.2 ka abrupt climate event
575 coincided with, and may have influenced, the transition between the Late Chalcolithic Los Millares
576 culture and the Early Bronze Age Argaric culture in southeast Iberia (Lull et al., 2015). However, it
577 had no detectable consequences for demographic trends in this sub-region, with inferred population
578 reaching a peak just after 4200 Cal yr BP. Nor does the pollen evidence analysed here indicate that
579 this short-lived dry phase had any clearly detectable direct consequences for vegetation in eastern
580 Iberia.

581

582 Human impact indicator groups are challenging to interpret for many Mediterranean regions, as
583 they include many taxa found within the natural vegetation. Patterns in these indicator groups are
584 simpler to interpret during the early Holocene prior to the first farming communities (when
585 vegetation is driven by climate and natural disturbance processes) and the late Holocene (when
586 vegetation is largely controlled by human transformation). Disentangling the relative importance of
587 natural and anthropogenic impact in the mid-Holocene is more difficult. Pollen diversity in all
588 regions is strongly related to radiocarbon-inferred population levels, and the NMDS chord distance
589 shows a strong relationship with prehistoric demography. This supports the assertion of Carrión et

590 al. (2010a) that human impacts should result in greater rates of change in vegetation. The analysis
591 presented here supports a role for climatic forcing of vegetation at the large scale, but clearly
592 demonstrates the importance of population changes in shaping the abundance and diversity of taxa
593 within broad biomes.

594

595 **ACKNOWLEDGEMENTS**

596

597 This research was funded by the Leverhulme Trust (grant RPG-2015-031). We thank all contributors
598 to the European Pollen Database for enabling access to published data and all those who have
599 compiled and archived archaeological radiocarbon dates from Iberia for their wider use by the
600 research community. We thank Shaun Lewin for assistance with extracting and formatting data
601 from the EPD. Thanks are extended to Joan Estrany and the University of the Balearic Islands for
602 hosting a workshop on Mallorca during which much of this work was discussed. This paper is a
603 contribution to the Past Global Change (PAGES) project and its LandCover6K working group, which
604 received support from the US National Science Foundation and the Swiss Academy of Sciences.

605

606 **REFERENCES**

607

608 Antolín F and Jacomet S (2015) Wild fruit use among early farmers in the Neolithic (5400-2300 cal
609 BC) in the north-east of the Iberian Peninsula: an intensive practice? *Vegetation History and*
610 *Archaeobotany* 24: 19-33.

611 Antolín F, Jacomet S and Buxó R (2015) The hard knock life. Archaeobotanical data on farming
612 practices during the Neolithic (5400-2300 cal BC) in the NE of the Iberian Peninsula. *Journal*
613 *of Archaeological Science* 61: 90-104

614 Aranbarri J, González-Sampériz P, Valero-Garcés B, Moreno A, Gil-Romera G, Sevilla-Callejo M,
615 García-Prieto E, Di Rita F, Mata MP, Morellón M, Magri D, Rodríguez-Lázaro J and Carrión JS
616 (2014) Rapid climatic changes and resilient vegetation during the Lateglacial and Holocene in
617 a continental region of south-west Europe. *Global and Planetary Change* 114, 50-65.

618 Aranda Jiménez G, Lozano Medina A and Sánchez Romero M (2015) CronoloGEA. Base de datos de
619 dataciones radiocarbónicas del sur de la Península Ibérica. Available at:
620 www.webgea.es/dataciones/ (accessed 01/05/2018)

621 Aranda Jiménez G, Montón-Subías S and Sánchez Romero M (2014) *The Archaeology of Bronze Age*
622 *Iberia: Argaric Societies*. Routledge.

623 Azuara J (2018) L'influence du climat et des activités humaines sur l'histoire Holocène de la
624 végétation du nord-ouest de la Méditerranée. PhD Thesis, Natural History Museum of Paris,
625 France.

626 Balsera V, Bernabeu Aubán J, Costa-Caramé M, Díaz-del-Río P, García Sanjuán L and Pardo-Gordó S
627 (2015a) The radiocarbon chronology of southern Spain's late prehistory (5600–1000 cal BC):
628 a comparative review. *Oxford Journal of Archaeology* 34: 139-156.

629 Balsera V, Díaz-del-Río P, Gilman A, Uriarte A and Vicent JM (2015b) Approaching the demography of
630 late prehistoric Iberia through summed calibrated date probability distributions (7000-2000
631 cal BC). *Quaternary International* 386: 208-211.

632 Bernabeu Aubán J, García Puchol O, Pardo-Gordó S, Barton M and McClure SB (2014) Socioecological
633 dynamics at the time of Neolithic transition in Iberia. *Environmental Archaeology* 19: 214-
634 225.

635 Bernabeu Aubán J, García Puchol O, Barton M, McClure S and Pardo-Gordó S (2016) Radiocarbon
636 dates, climatic events, and social dynamics during the Early Neolithic in Mediterranean
637 Iberia. *Quaternary International* 403: 201-210.

638 Bevan A, Colledge S, Fuller D, Fyfe R, Shennan S and Stevens C (2017) Holocene fluctuations in
639 population demonstrate repeated links to food production and climate. *PNAS* E10524-
640 E10531

641 Blaauw M and Christen JA (2011) Flexible paleoclimate age-depth models using an autoregressive
642 gamma process. *Bayesian Analysis* 6: 457-474.

643 Blanco-González A, Lillios KT, López-Sáez JA and Drake BL (2018) Cultural, demographic and
644 environmental dynamics of the Copper and early Bronze Age in Iberia (3300-1500 BC):
645 towards and interregional multiproxy comparison at the time of the 4.2 ky BP event. *Journal*
646 *of World Prehistory* 31: 1-79.

647 Burjachs F (2006) Palinología y restitución palinológica. *Ecosistemas - Revista Científica y Técnica e*
648 *Ecología y Medio Ambiente* 15, 1-10.

649 Burjachs F and Expósito I (2015) Charcoal and pollen analysis: Examples of Holocene fire dynamics in
650 Mediterranean Iberian Peninsula. *Catena* 135: 340-349.

651 Burjachs F, Jones SE, Giralt S and Fernández-López de Pablo J (2016) Lateglacial to Early Holocene
652 recursive aridity events in the SE Mediterranean Iberian Peninsula: The Salines playa lake
653 case study. *Quaternary International* 403: 187-200.

654 Burjachs F, Giralt S, Roca JR, Seret G and Julià R (1997) Palinología holocena y desertización en el
655 Mediterráneo Occidental. In: Ibáñez JJ, Valero BI and Machado C (eds) *El paisaje*

656 *Mediterráneo a través del espacio y del tiempo. Implicaciones en la desertificación*, Logroño:
657 Geoforma Ediciones, 379–394.

658 Burjachs F, Pérez-Obiol R, Picornell-Gelabert L, Revelles J, Servera-Vives G, Expósito I, Yll E-I (2017)
659 Overview of environmental changes and human colonisation in the Balearic Islands (Western
660 Mediterranean) and their impacts on vegetation composition during the Holocene. *Journal*
661 *of Archaeological Science: Reports* 12: 845-859.

662 Burjachs F, Pérez-Obiol R, Roure JM and Julià, R (1994) Dinámica de la vegetación durante el
663 Holoceno en la isla de Mallorca. *Trabajos de Palinología básica y aplicada*, 199-210.

664 Burjachs F and Schulte L (2003) El paisatge vegetal del Penedès entre la Prehistòria i el Món Antic. In:
665 Guitart J, Palet JM and Prevosti M (eds) *Territoris antics a la Mediterrània i a la Cossetània*
666 *oriental*, Barcelona: Direcció General del Patrimoni Cultural, Servei d'Arqueologia,
667 Departament de Cultura, Generalitat de Catalunya, 249-254.

668 Carrión JS (2002) Patterns and processes of Late Quaternary environmental change in a montane
669 region of southwestern Europe. *Quaternary Science Reviews* 21: 2047-2066.

670 Carrión JS (2012) *Paleoflora y Paleovegetación de la Península Ibérica e Islas Baleares: Plioceno-*
671 *Cuaternario*. Madrid: Ministerio de Economía y Competitividad.

672 Carrión JS, Andrade A, Bennett KD, Navarro C and Munuera M (2001a) Crossing forest thresholds:
673 inertia and collapse in a Holocene sequence from south-central Spain. *The Holocene* 11: 635-
674 653.

675 Carrión JS and Dupré-Olivier M (1996) Late Quaternary vegetational history of Navarrés, eastern
676 Spain. A two core approach. *New Phytologist* 134: 177-191.

677 Carrión JS, Fernández S, González-Sampérez P, Gil-Romera G, Badal E, Carrión-Marco Y, López-Merino
678 L, López-Sáez JA, Fierro E and Burjachs F (2010a) Expected trends and surprises in the
679 Lateglacial and Holocene vegetation history of the Iberian Peninsula and Balearic Islands.
680 *Review of Palaeobotany and Palynology* 162: 458-475.

681 Carrión JS, Fernández S, Jiménez-Moreno G, Fauquette S, Gil-Romera G, González-Sampérez P and
682 Finlayson C (2010b) The historical origins of aridity and vegetation degradation in
683 southeastern Spain. *Journal of Arid Environments* 74: 731-736.

684 Carrión JS, Fuentes N, González-Sampérez P, Sánchez Quirante L, Finlayson JC, Fernández S and
685 Andrade A (2007) Holocene environmental change in a montane region of southern Europe
686 with a long history of human settlement. *Quaternary Science Reviews* 26: 1455-1475.

687 Carrión JS, Munuera M, Dupré M and Andrade A (2001b) Abrupt vegetation changes in the Segura
688 Mountains of southern Spain throughout the Holocene. *Journal of Ecology* 89: 783-797.

689 Carrión JS, Sánchez-Gómez P, Mota JF, Yll EI and Chaín C (2003) Fire and grazing are contingent on
690 the Holocene vegetation dynamics of Sierra de Gádor, southern Spain. *The Holocene* 13: 839-
691 849.

692 Carrión JS and van Geel B (1999) Fine-resolution Upper Weichselian and Holocene palynological
693 record from Navarrés (Valencia, Spain) and a discussion about factors of Mediterranean
694 forest succession. *Review of Palaeobotany and Palynology* 106: 209-236.

695 Carrión JS, Yll E-I, Willis KJ and Sánchez P (2004) Holocene forest history of the eastern plateaux in
696 the Segura Mountains (Murcia, southeastern Spain). *Review of Palaeobotany and Palynology*
697 132: 219-236.

698 Castro P, Chapman R, Gili S, Lull V, Micó R and Rihuete C (1998) *Aguas Project. Palaeoclimatic*
699 *reconstruction and the dynamics of human settlement and land use in the area of the middle*
700 *Aguas (Almería) in the south-east of the Iberian Peninsula*. Luxemburg: European
701 Commission.

702 Castro PEC, Courty MA, Federoff N, Gili S and González Marcén P (1994). *Temporalities and*
703 *desertification in the Vera Basin, south-east Spain (Vol. 2)*. Brussels: Archaeomedes Project.

704 Cortés-Sánchez M, Espejo FJJ, Vallejo MDS, Bao JFG, Carvalho AF, Martínez-Ruiz F, Gamiz MR, Flores
705 JA, Paytan A, López-Sáez JA and Peña-Chocarro L (2012). The Mesolithic–Neolithic transition
706 in southern Iberia. *Quaternary Research* 77: 221-234.

707 Crema ER, Habu J, Kobayashi K and Madella M (2016) Summed probability distribution of 14C dates
708 suggests regional divergences in the population dynamics of the Jomon period in eastern
709 Japan. *PLoS One* 11: e0154809.

710 Davis BA and Stevenson AC (2007) The 8.2 ka event and Early–Mid Holocene forests, fires and
711 flooding in the Central Ebro Desert, NE Spain. *Quaternary Science Reviews* 26: 1695-1712.

712 Davis BAS, Zanon M, Collins P, Mauri A, Bakker J, Barboni D, Barthelmes A, Beaudouin C, Birks, HJB,
713 Bjune AE, Bozilova E, Bradshaw RHW, Brayshay BA, Brewer S, Brugiapaglia E, Bunting J,
714 Conner SE, de Beaulieu J-L, Edwards KJ, Ejarque A, Fall P, Florenzano A, Fyfe R, Galop D,
715 Giardini M, Giesecke T, Grant MJ, Guiot J, Jahns S, Jankovská V, Juggins S, Karmann M,
716 Karpinska-Kolaczek M, Kolaczek P, Kuhl N, Kunes P, Lapteva EG, Leroy SAG, Leydet M, López-
717 Sáez JA, Masi A, Matthias I, Mazier F, Meltsov V, Mercuri AM, Miras Y, Mitchell FJG, Morris
718 JL, Naughton F, Nielsen AB, Novenko E, Odgaard B, Ortu E, Overballe-Petersen MV, Pardoe
719 HS, Peglar SM, Pidek I, Sadori L, Seppa H, Severova E, Shaw H, Swieta-Musznicka J,
720 Theuerkauf M, Tonkov S, Veski S, van der Knaap WO, van Leeuwen J, Woodbridge J, Zimny M
721 and Kaplan JO (2013) The European Modern Pollen Database (EMPD) project. *Vegetation*
722 *History and Archaeobotany* 22: 521-530.

723 Drake BL, Blanco-González A and Lillios KT (2017) Regional demographic dynamics in the Neolithic
724 transition in Iberia: results from summed calibrated data analysis. *Journal of Archaeological*
725 *Method and Theory* 24: 796-812.

726 Fernández-López de Pablo JF and Gómez-Puche M (2009) Climate change and population dynamics
727 during the Late Mesolithic and the Neolithic transition in Iberia. *Documenta Praehistorica* 36:
728 67-96.

729 Fyfe RM, Woodbridge J and Roberts CN (2018) Trajectories of change in Mediterranean Holocene
730 vegetation through classification of pollen data. *Vegetation History and Archaeobotany* 27:
731 351-364.

732 García Puchol O, Castillo AD and Pardo Gordó S (2017) New insights in the neolithization process in
733 southwest Europe according to spatial density analysis from calibrated radiocarbon dates.
734 *Archaeological and Anthropological Sciences* 9: 1-14.

735 García Puchol O, Molina Balaguer L, Aura Tortosa JE and Bernabeu Aubán J (2009). From the
736 Mesolithic to the Neolithic on the Mediterranean Coast of the Iberian Peninsula. *Journal of*
737 *Anthropological Research* 65: 237-251.

738 García Puchol O and Salazar-García DC (2017) *Times of Neolithic transition along the western*
739 *Mediterranean* Springer International.

740 Giesecke T, Davis B, Brewer B, Finsinger W, Wolters S, Blaauw M, de Beaulieu J-L, Fyfe RM, Gaillard
741 M-J, Gil-Romera G, van der Knaap WO, Kuneš P, Kühl N, van Leeuwen JFN, Leydet M, Lotter
742 AF, Semmler M and Bradshaw RHW (2014) Towards mapping the late Quaternary vegetation
743 change of Europe. *Vegetation History and Archaeobotany* 23: 75-86.

744 Giralt S, Burjachs F, Roca JR, Julià R (1999) Late Glacial to Early Holocene environmental adjustment
745 in the Mediterranean semi-arid zone of the Salines playa-lake (Alacant, Spain). *Journal of*
746 *Paleolimnology* 21: 449–460.

747 Hinz M, Furholt M, Müller J, Raetzl-Fabian D, Rinne C, Sjögren K-G and Wotzka HP (2012)
748 Radiocarbon dates online 2012. Central European database of ¹⁴C dates for the Neolithic and
749 Early Bronze Age. Available at: www.jungsteinsite.de (accessed 01/05/2018)

750 Juggins S (2015) 'Rioja': Analysis of Quaternary Science Data, R package version (0.9-9).
751 (<http://cran.r-project.org/package=rioja>).

752 Leydet M (2007-2017) *The European Pollen Database*. (online:
753 <http://www.europeanpollendatabase.net/>). Accessed: Oct. 2017.

754 Lillios KT, Blanco-González A, Drake BL and López-Sáez JA (2016) Mid-late Holocene climate,
755 demography, and cultural dynamics in Iberia: a multi-proxy approach. *Quaternary Science*
756 *Reviews* 135: 138-153.

757 Lull V, Micó R, Herrada CR and Risch R (2013) Bronze Age Iberia. In: Harding A and Fokkens H (eds)
758 *The Oxford Handbook of the European Bronze Age*. Oxford: Oxford University Press, pp.596-
759 616.

760 Lull V, Micó R, Rihuete C and Risch R (2015) Transition and conflict at the end of the 3rd millennium
761 BC in Southern Iberia. In: Meller H, Arz HW, Jung R and Risch R(eds) *2200 BC - a climatic
762 breakdown as a cause for the collapse of the Old World?* Halle, 365-407.

763 Manen C and Sabatier P (2003) Chronique radiocarbone de la néolithisation en Méditerranée nord-
764 occidentale. *Bulletin de la Société Préhistorique Française* 100: 479-504.

765 Manning K, Timpson A, Colledge S, Crema E, Shennan S (2015) The cultural evolution of Neolithic
766 Europe. EUROEVOL dataset. Available at: <http://discovery.ucl.ac.uk/1469811/> (accessed
767 01/05/2018)

768 Martínez PVC, Suriñach SG, Marcén PG, Lull V, Pérez RM and Herrada CR (1997) Radiocarbon dating
769 and the prehistory of the Balearic Islands. *Proceedings of the Prehistoric Society* 63: 55-86.

770 Mercuri AM, Bandini Mazzanti M, Florenzano A, Montecchi MC and Rattighieri E (2013a) Olea,
771 Juglans and Castanea: the OJC group as pollen evidence of the development of human-
772 induced environments in the Italian peninsula. *Quaternary International* 303: 24-42.

773 Mercuri AM, Mazzanti M, Florenzano A, Montecchi MC, Rattighieri E and Torri P (2013b)
774 Anthropogenic pollen indicators (API) from archaeological sites as local evidence of human-
775 induced environments in the Italian peninsula. *Annali Di Botanica* 3: 143-153.

776 Morellón M, Valero-Garcés B, Vegas-Vilarrúbia T, González-Sampériz P, Romera O, Delgado-Huertas
777 A, Mata P, Moreno A, Rico M and Corella JP (2009) Lateglacial and Holocene
778 palaeohydrology in the western Mediterranean region: the Lake Estanya record (NE Spain).
779 *Quaternary Science Reviews* 28: 2582-2599.

780 Murillo-Barroso M, Martín-Torres M, Massieu MDC, Socas DM and González FM (2017) Early
781 metallurgy in SE Iberia. The workshop of Las Pilas (Mojácar, Almería, Spain). *Archaeological
782 and Anthropological Sciences* 9: 1-31.

783 Oms FX, Martín A, Esteve X, Mestres J, Morell B, Subirà ME and Gibaja JF (2016) The Neolithic in
784 Northeast Iberia: Chronocultural Phases and 14C. *Radiocarbon* 58: 291-309.

785 Oms FX, Terrades X, Morell B and Gibaja JF (2018) Mesolithic-Neolithic transition in the northeast of
786 Iberia: chronology and socioeconomic dynamics. *Quaternary International* 470: 383-397.

787 Oksanen J, Blanchet FG, Friendly M, Kindt R, Legendre P, McGlenn D, Minchin, PR, O'Hara RB,
788 Simpson GL, Solymos P, Stevens MHH, Szoecs E and Wagner H (2016) Vegan: Community
789 Ecology Package. R package version 2.4-1. <https://CRAN.R-project.org/package=vegan>.

790 Palmisano A, Bevan A and Shennan S (2017) Comparing archaeological proxies for long-term
791 population patterns: an example from central Italy. *Journal of Archaeological Science* 87: 59-
792 72.

793 Pantaleón-Cano J, Yll EI, Pérez-Obiol RP and Roure JM (2003) Palynological evidence for vegetational
794 history in semi-arid areas of the western Mediterranean (Almeria, Spain). *The Holocene* 13:
795 109-119.

796 Paulsson B (2017) *Time and Stone, The Emergence and Development of Megaliths and Megalithic*
797 *Societies in Europe*. Oxford: Archaeopress.

798 Pérez-Jordá G, Peña-Chocarro L, Picornell-Gelabert L and Carrión Marco Y (2018) Agriculture
799 between the third and first millennium BC in the Balearic Islands: the archaeobotanical data.
800 *Vegetation History and Archaeobotany* 27: 253-265.

801 Pérez-Obiol R (2007) Palynological evidence for climatic change along the eastern Iberian Peninsula
802 and Balearic Islands. *Contributions to Science* 3: 415-419.

803 Pérez-Obiol R, Jalut G, Julià R, Pèlachs A, Iriarte MJ, Otto T and Hernández-Beloqui B (2011) Mid-
804 Holocene vegetation and climatic history of the Iberian Peninsula. *The Holocene* 21: 75-93.

805 Pérez-Obiol RP and Julià R (1994) Climatic change on the Iberian Peninsula recorded in a 30,000-year
806 pollen record from Lake Banyoles. *Quaternary Research* 41: 91-98.

807 Ramis D, Alcover JA, Coll J and Trias M (2002) The chronology of the first settlement of the Balearic
808 Islands. *Journal of Mediterranean Archaeology* 15: 3-24.

809 Reed JM, Stevenson AC and Juggins S (2001) A multi-proxy record of Holocene climatic change in
810 southwestern Spain: the Laguna de Medina, Cádiz. *The Holocene* 11: 707-719.

811 Revelles J, Cho S, Iriarte E, Burjachs F, van Geel B, Palomo A, Piqué R, Peña-Chocarro L and Terradas
812 X (2015) Mid-Holocene vegetation history and Neolithic land-use in the Lake Banyoles area
813 (Gironde, Spain). *Palaeogeography, Palaeoclimatology, Palaeoecology* 435: 70-85.

814 Rodríguez-Ariza MO and Montes Moya E (2005) On the origin and domestication of *Olea europaea* L.
815 (olive) in Andalucía, Spain, based on the biogeographical distribution of its finds. *Vegetation*
816 *History and Archaeobotany* 14: 551-561.

817 Rowley-Conwy P and Layton R (2011) Foraging and farming as niche construction: stable and
818 unstable adaptation. *Philosophical Transactions of the Royal Society B* 366: 849-862.

819 Shennan S, Downey SS, Timpson A, Edinborough K, Colledge S, Kerig T, Manning K and Thomas MG
820 (2013) Regional population collapse followed initial agricultural booms in mid-Holocene
821 Europe. *Nature Communications* 4: article number 2486.

822 Shennan S and Edinborough K (2007) Prehistoric population history: from the Late Glacial to the Late
823 Neolithic in Central and Northern Europe. *Journal of Archaeological Science* 34: 1339-1345.

- 824 Silvertown J (1985) History of a latitudinal diversity gradient: woody plants in Europe 13000-1000
825 years BP. *Journal of Biogeography* 12: 519-525.
- 826 Simpson EH (1949) Measurement of diversity. *Nature* 163: 688.
- 827 Terral JF and Arnold-Simard G (1996) Beginnings of olive cultivation in eastern Spain in relation to
828 Holocene bioclimatic changes. *Quaternary Research* 46: 176-185.
- 829 Timpson A, Colledge S, Crema E, Edinborough K, Kerig T, Manning K, Thomas MG and Shennan S
830 (2014) Reconstructing regional population fluctuations in the European Neolithic using
831 radiocarbon dates: a new case-study using an improved method. *Journal of Archaeological
832 Science* 52: 549-557.
- 833 Van Strydonck M and De Roock E (2011) Royal Institute for Cultural Heritage web-based radiocarbon
834 database. *Radiocarbon* 53: 367-370.
- 835 Vermeersch PM (2017) Radiocarbon Palaeolithic Europe Database. Version 23. Available at:
836 <http://ees.kuleuven.be/geography/projects/14c-palaeolithic/index.html> (accessed
837 01/05/2018).
- 838 Ward JH (1963) Hierarchical grouping to optimize an objective function. *Journal of the American
839 Statistical Association* 58: 236-244.
- 840 Weninger B, Edinborough K, Bradtmöller M, Collard M, Crombé P, Danzeglocke U, Holst D, Jöris O,
841 Niekus M, Shennan S and Schulting R (2009) A radiocarbon database for the Mesolithic and
842 early Neolithic in Northwest Europe. In Crombé P, van Strydonck M, Sergant J, Boundin M
843 and Bats M (eds) *Chronology and evolution within the Mesolithic of North-West Europe*.
844 Cambridge: Cambridge Scholars Publishing, pp. 143-176.
- 845 Woodbridge J, Roberts CN and Fyfe RM (2018) Pan-Mediterranean Holocene vegetation and land-
846 cover dynamics from synthesised pollen data *Journal of Biogeography* DOI: 10.1111/jbi.13379
- 847 Yll EI, Pérez-Obiol R, Pantaleón-Cano J and Roure JM (1995) Dinámica del paisaje vegetal en la
848 vertiente mediterránea de la Península Ibérica e Islas Baleares desde el Tardiglacial hasta el
849 presente. *Reconstrucción de Paleoambientes y cambios climáticos durante el Cuaternario* 3:
850 319-328.
- 851 Yll EI, Pérez-Obiol R, Pantaleón-Cano J and Roure JM (1997) Palynological evidence for climatic
852 change and human activity during the Holocene on Minorca (Balearic Islands). *Quaternary
853 Research* 48: 339-347.

854 Table 1: sites used within the Spain case study analysis *indicates dataset from the EPD

Site#	SiteName	site code	LatDD	LonDD	Elevation	Region	References/contributor
1	Amposta	AMPOSTA	40.704	0.597	5	NESpain	Pérez-Obiol 2007, Pérez-Obiol et al 2011
2	Creixell	CREIXELL	41.166	1.440	5	NESpain	Burjachs and Schulte 2003, Carrión 2012, Burjachs and Expósito 2015
3	Laguna Salada Chiprana*	N-SAL	41.233	-0.166	150	NESpain	EPD dataset: no citation
4	Lake Banyoles* Banyoles SB2	BANYOLES	42.133	2.750	175	NESpain	Pérez-Obiol and Julià 1994 Revelles et al 2015
5	Hoya del Castillo*	N-CAS	41.250	-0.500	250	NESpain	Davis and Stevenson 2007
6	Laguna Guallar*	N-GUA	41.400	-0.216	330	NESpain	Davis and Stevenson 2007
7	Salada Pequeña*	N-PEQ	41.033	-0.216	360	NESpain	EPD dataset: no citation
8	Roquetas de Mar*	ROQUETAS	36.7944	-2.588	5	SESpain	Pantaleón-Cano et al 2003
9	San Rafael*	SANRAFA	36.773	-2.601	5	SESpain	Pantaleón-Cano et al 2003
10	Elx (Alacant)	ELX	38.174	-0.752	10	SESpain	Burjachs et al 1997, Carrión 2012
11	Antas*	ANTAS	37.208	-1.823	10	SESpain	Pantaleón-Cano et al 2003
12	Navarrés *	NAVARRES, NAVA 1+2, NAVARRE3	39.070	-0.680	225	SESpain	Carrión and Dupré-Olivier 1996; Carrión and van Geel 1999
13	Salines (Alacant)	SALINES	38.500	-0.888	500	SESpain	Giralt et al 1999, Carrión 2012, Burjachs et al 2016
14	Villaverde	VILLAVERDE	38.800	-2.220	890	SESpain	Carrión et al 2001a
15	Siles	SILES	38.440	-2.510	1050	SESpain	Carrión et al 2001b
16	Sabinar	SABINAR	38.200	-2.116	1130	SESpain	Carrión et al 2004
17	Gador	GADOR	36.930	-2.910	1650	SESpain	Carrión et al 2003
18	Cañada de la Cruz	CANADACRUZ	38.066	-2.700	1650	SESpain	Carrión et al 2001b
19	Baza	BAZA	37.233	-2.700	1850	SESpain	Carrión et al 2007
20	Prat de Vila (Eivissa)	PRATDEVILA	38.915	1.435	5	Balearic	Burjachs et al 2017
21	Albufera Alcúdia (Majorque)*	ALCUDIA	39.792	3.119	5	Balearic	Burjachs et al 1994, Burjachs et al 2017
22	Es Grau (Menorca)	ESGRAU	39.948	4.258	30	Balearic	Burjachs 2006
23	Son Bou*	SONBOU	39.924	4.027	15	Balearic	Yll et al 1997
24	Algendar*	ALGENDAR	39.940	3.958	20	Balearic	Yll et al 1995
25	Cala'n Porter*	CPORTER	39.870	4.131	25	Balearic	Yll et al 1997
26	Hort Timoner*	HTIMONER	39.875	4.126	40	Balearic	Yll et al 1997
27	Cala Galdana*	GALDANA	39.900	4.000	50	Balearic	Yll et al 1995
A	Laguna de Medina	-				SESpain	Reed et al 2001
B	Lake Estanya	-				NESpain	Morellón et al 2009

856 Table 2: Northeast Spain Spearman's Rank Correlation Coefficient r-value matrix for the period
 857 10000-2500 cal. yr BP. Shaded boxes indicate p<0.05.

	14C SPD	NMDS chord distance	NAP sum	OJC index	API	Simpson's diversity	Estanya z- score
14C SPD	1.000	0.269	0.647	0.408	0.324	0.287	-0.013
NMDS chord distance		1.000	0.228	0.031	0.128	0.092	-0.009
NAP sum			1.000	0.415	0.747	0.607	0.029
OJC index				1.000	0.265	0.521	-0.153
API					1.000	0.424	0.0153
Simpson's diversity						1.000	-0.265
Estanya z-score							1.000

858

859 Table 3: Southeast Spain Spearman's Rank Correlation Coefficient r-value matrix for the period 9000-
 860 2500 cal. yr BP. Shaded boxes indicate $p < 0.05$.

	14C SPD	NMDS chord distance	NAP sum	OJC index	API	Simpson's diversity	Laguna de Medina z- score
14C SPD	1.000	0.338	0.008	-0.585	-0.152	0.387	0.115
NMDS chord distance		1.000	0.035	-0.220	-0.090	0.156	0.135
NAP sum			1.000	-0.322	0.466	0.431	0.232
OJC index				1.000	-0.073	-0.354	-0.189
API					1.000	0.068	0.098
Simpson's diversity						1.000	0.073
Laguna de Medina z-score							1.000

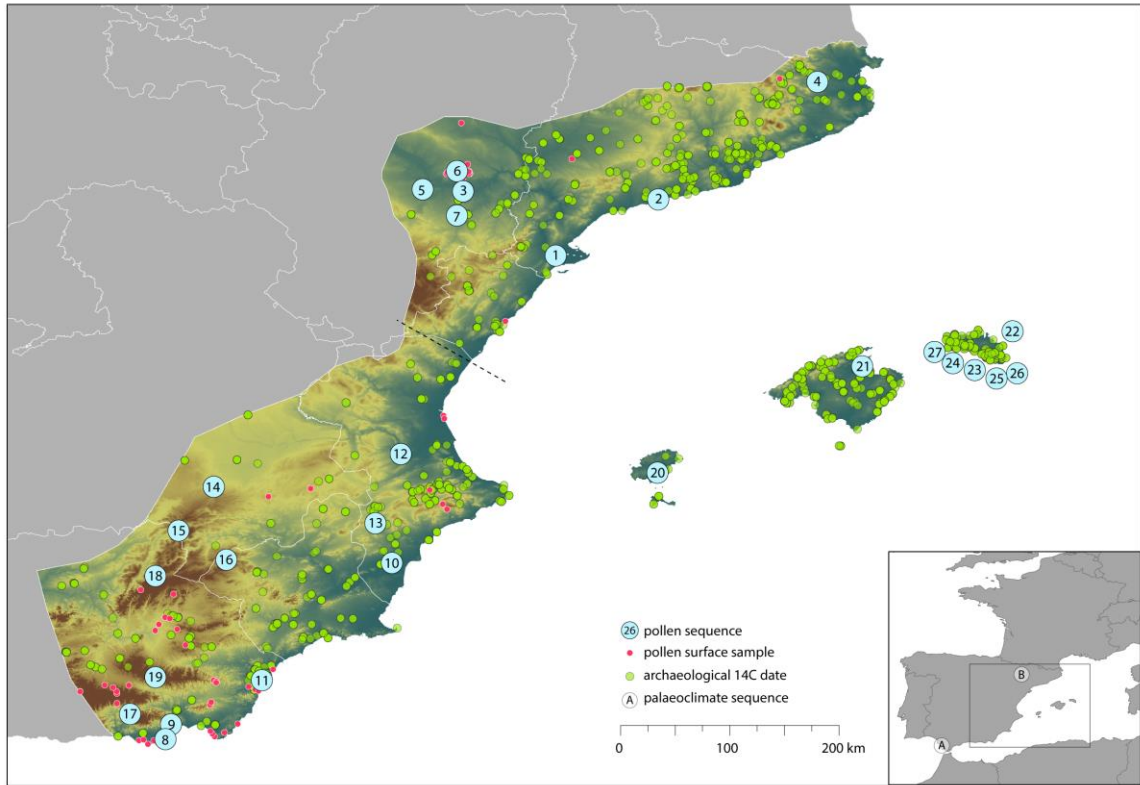
861

862 Table 4: Balearic Islands Spearman's Rank Correlation Coefficient r-value matrix for the period 9000-
 863 2000 cal. yr BP. Shaded boxes indicate $p < 0.05$.

	14C SPD	nMDS chord distance	NAP sum	OJC index	API	Simpson's diversity
14C SPD	1.000	-0.095	0.739	0.734	-0.214	0.345
nMDS chord distance		1.000	-0.300	0.019	-0.313	0.049
NAP sum			1.000	0.762	0.306	0.438
OJC index				1.000	0.138	0.435
API					1.000	0.025
Simpson's diversity						1.000

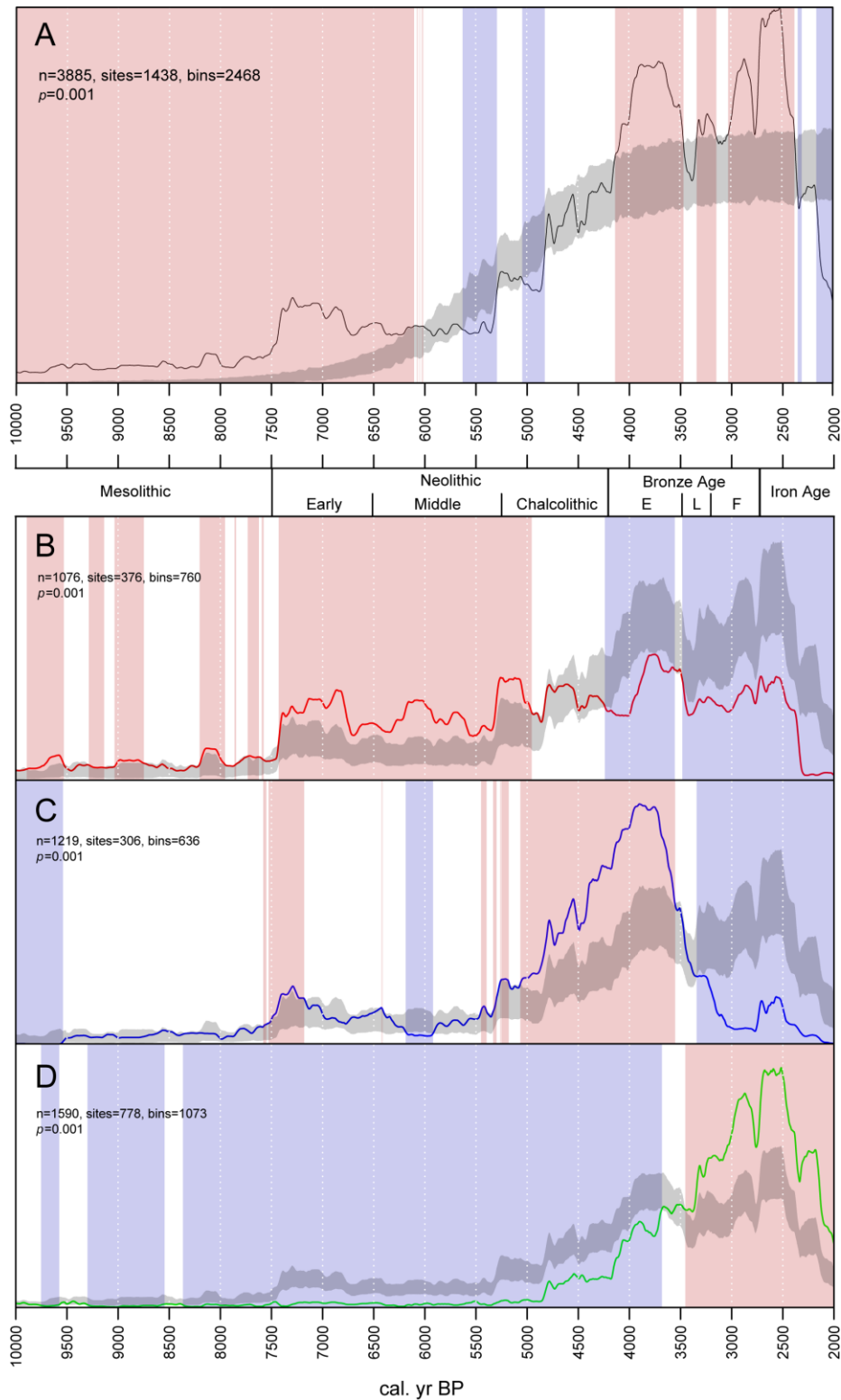
864

865 Figure 1: location of pollen samples (sub-fossil and surface samples) and archaeological radiocarbon
866 dates used within the analysis. The division between northeast and southeast Spain is indicated by
867 the dashed line. Pollen site numbers are the same as those in Table 1. Palaeoclimate sequences: (A)
868 Laguna de Medina (Reed et al. 2001); (B) Lake Estanya (Morellón et al. 2009).



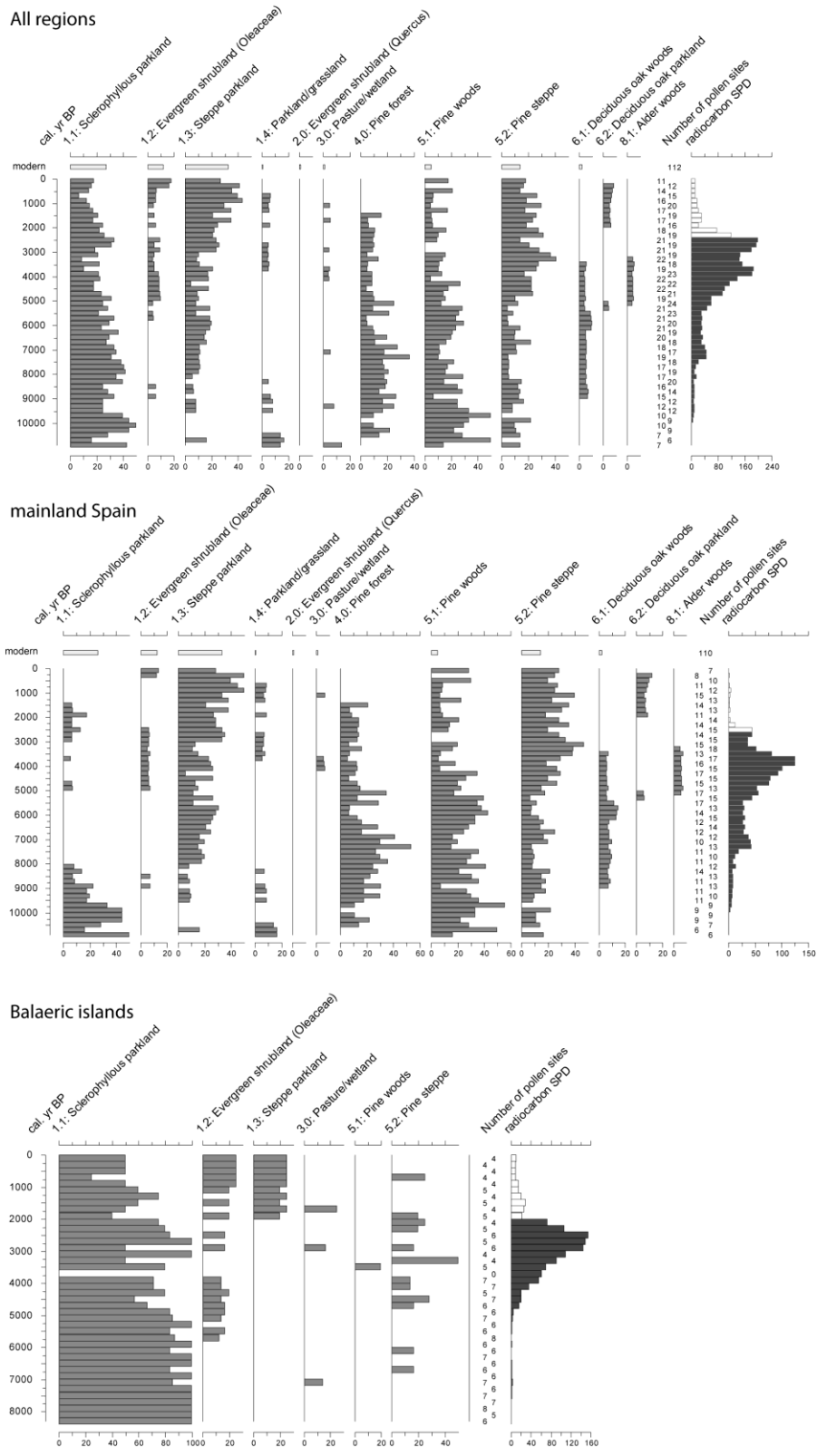
869

870 Figure 2: Summed Probability Distributions (SDP) of un-normalised calibrated radiocarbon dates (cal.
 871 yr BP). A: all radiocarbon dates against a fitted logistic model (95% confidence); B: north-east Spain,
 872 with SDP for all eastern Spain dates; C: south-east Spain, with SDP for all Spain dates; D: Balearic
 873 Islands, with SDP for all Spain dates. Vertical bands indicate negative or positive deviations from the
 874 null model (panel A) or all Spain dates (B-D).



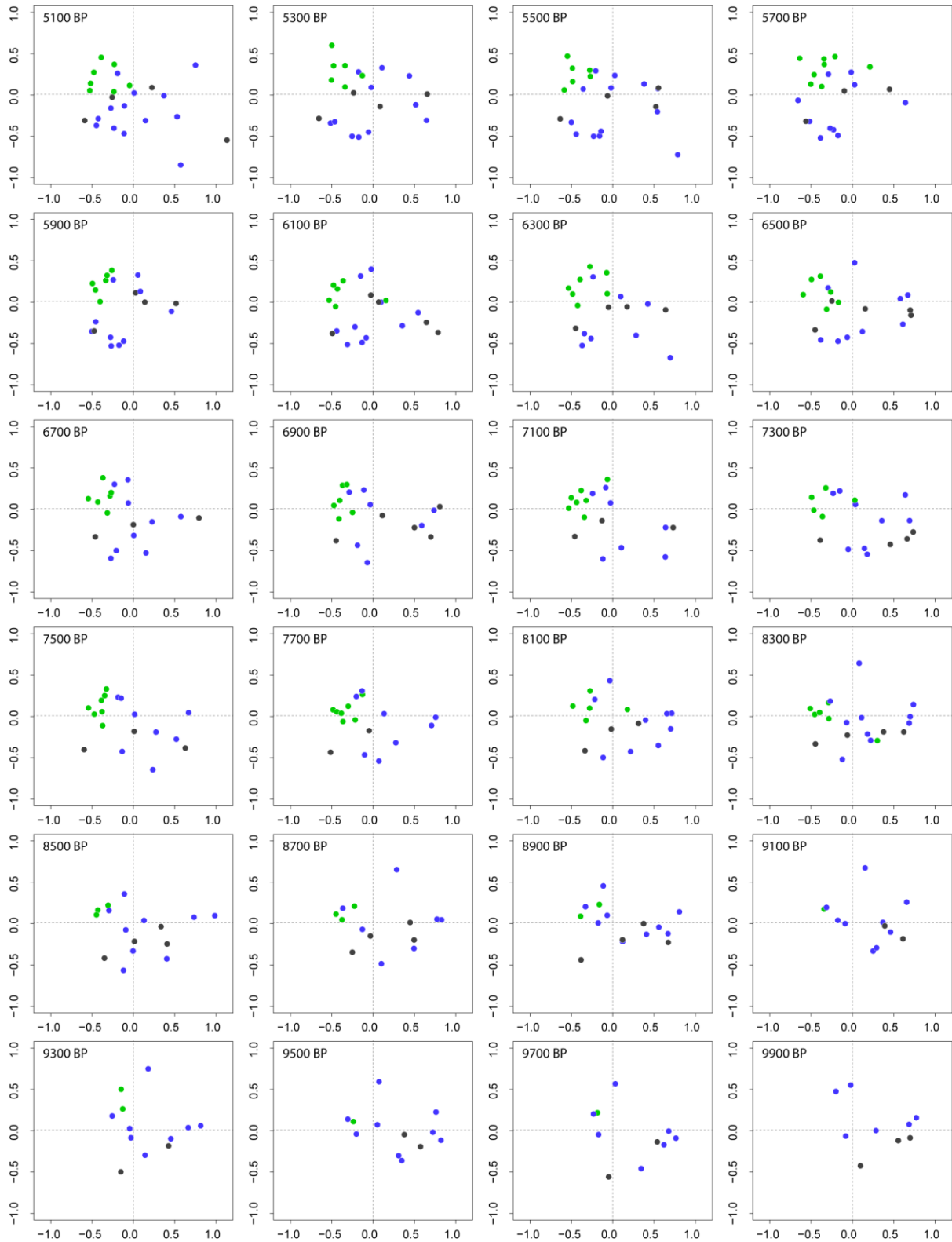
875

876 Figure 3: relative proportions of pollen samples within each vegetation cluster in each time window,
 877 for (A) all sites, (B) sites on mainland Spain (northeast and southeast regions combined) and (C)
 878 Balearic Islands. Radiocarbon summed probability distributions show results for all dates collated.
 879 Time windows with insufficient radiocarbon dates for reliable SDP are shown in white.

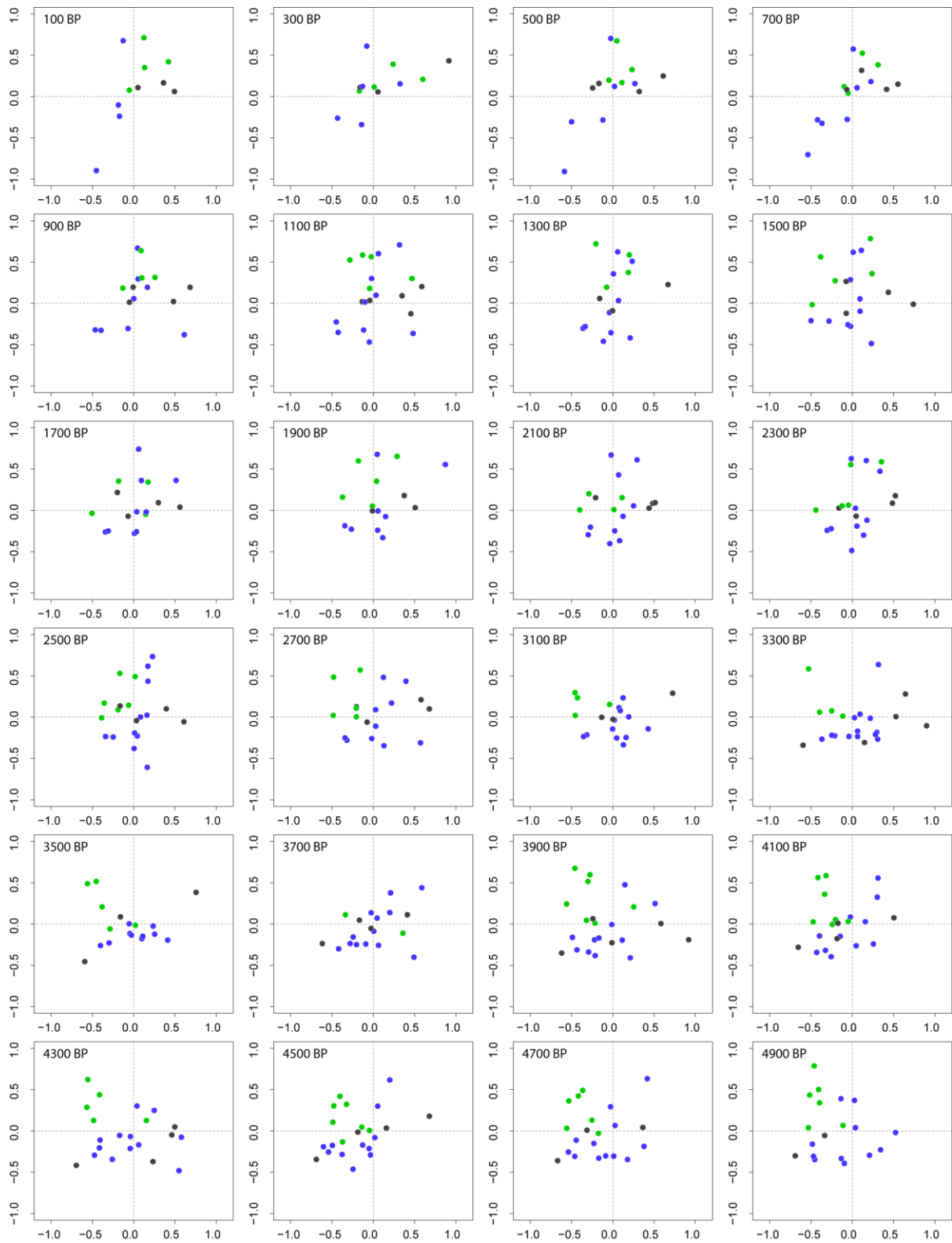


880

885 Figure 5: site plots from non-metric multidimensional scaling (NMDS) analysis in each time interval.
 886 (A) 9900-5100 cal. yr BP; (B): 4900-100 cal. yr BP. Plot shows axis 1 vs 2 scores. Green is Balearic
 887 sites, black northeast Spanish sites and blue southeast Spanish sites. [labelled version in
 888 Supplementary Information]



889 ● northeast sites ● southeast sites ● Balearic sites

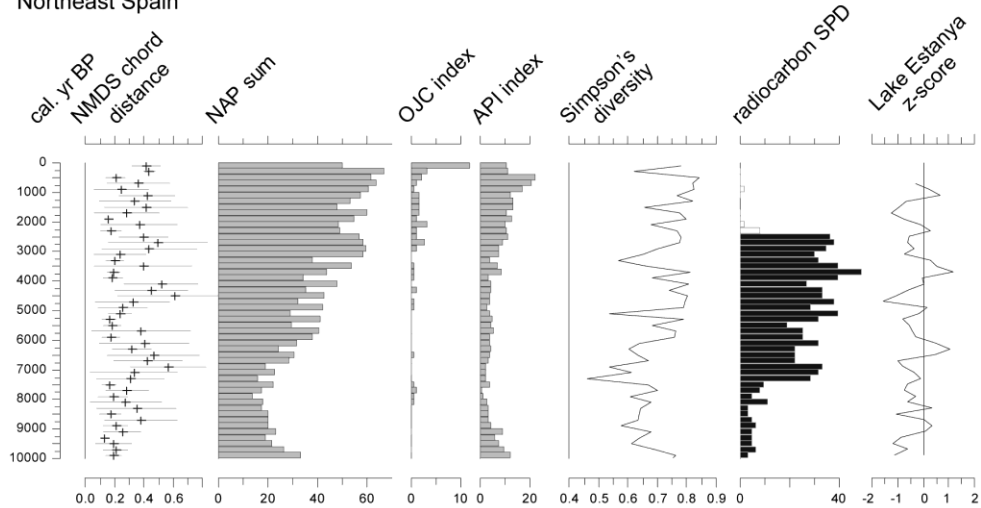


890

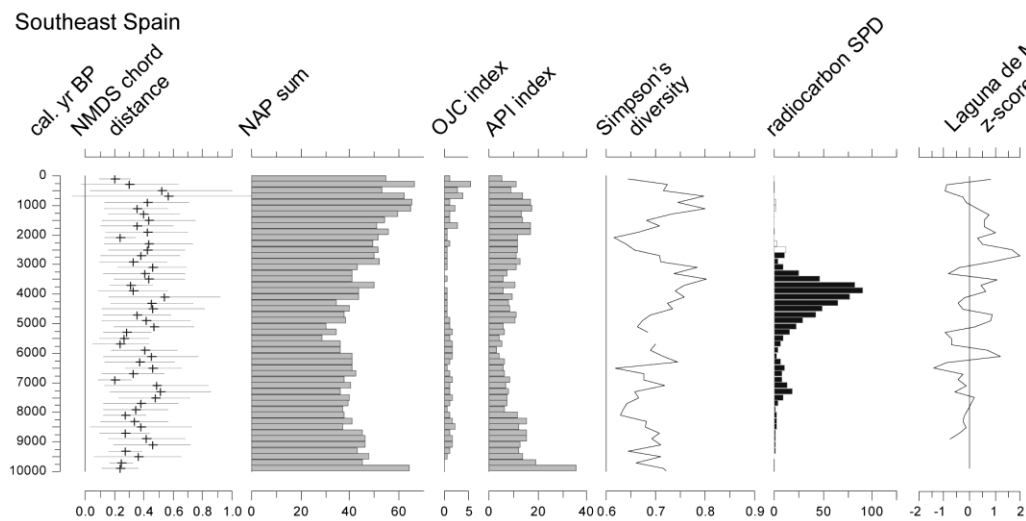
● northeast sites ● southeast sites ● Balearic sites

891 Figure 6: regional plots of pollen assemblage change (mean NMDS chord distance), sum of non-
 892 arboreal pollen types, key anthropogenic indicator groups (API and OJC), Simpson's diversity index,
 893 radiocarbon summed probability distributions for each region and z-scores for regional proxy-
 894 climate records (Lake Estanya: Morellón et al 2009; Laguna de Medina: Reed et al 2001).

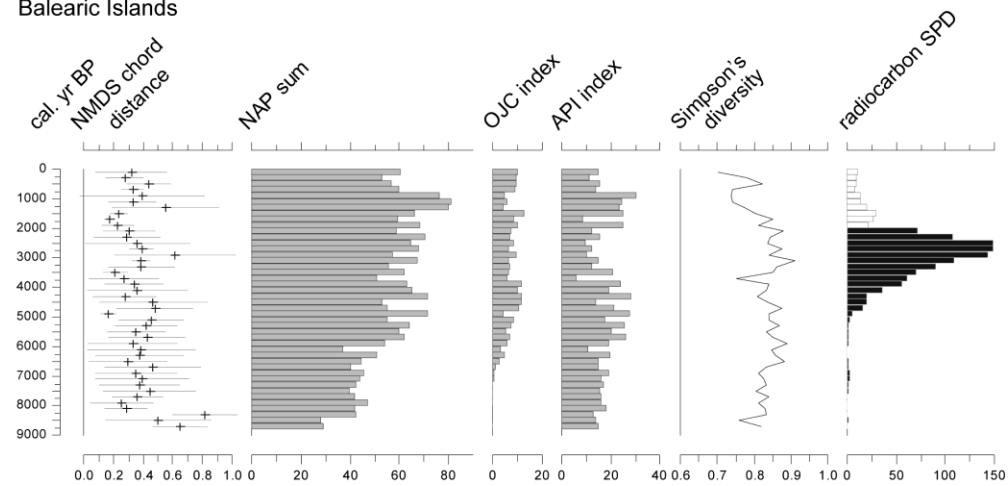
Northeast Spain



Southeast Spain



Balearic Islands



895